

Combining hydrogen bonds with coordination chemistry or organometallic π -arene chemistry: strategies for inorganic crystal engineering †

Lee Brammer,* Juan C. Mareque Rivas,‡ Reinaldo Atencio,§ Shiyue Fang and F. Christopher Pigge

Department of Chemistry, University of Missouri-St. Louis, 8001 Natural Bridge Road, St. Louis, MO 63121-4499, USA. E-mail: lee.brammer@umsl.edu

Received 1st June 2000, Accepted 20th July 2000

First published as an Advance Article on the web 2nd October 2000

Two strategies are described for the construction of extended arrays of transition metal-containing molecules linked *via* hydrogen bonds. The first approach connects the transition metal to the ligand bearing the hydrogen-bonding group(s) *via* a coordinative bond. Thus, coordination complexes with peripheral hydrogen-bonding functional groups constitute the (molecular) building blocks of the assembly. The ligands, substituted pyridines, have been selected to provide rigidity and thus permit the metal coordination geometry to guide the direction of propagation of the hydrogen-bonded links between building blocks. The second approach uses arenes bearing hydrogen-bonding functional groups, the arenes being π -bound to transition metals as is typical of sandwich and half-sandwich organometallic compounds. In the first approach the metal can be viewed as serving a directing role in propagation of the hydrogen bonded assembly. In the second, the metal can be thought of as a (potentially functional) appendage to an organic hydrogen-bonded array, where substituent position at the arene ring serves the directing role for propagation. Examples presented for discussion of the coordination chemistry approach are compounds of the form $[\text{PtL}_4]\text{X}_2$ (L = nicotinamide or isonicotinamide; $\text{X}^- = \text{Cl}^-$ or PF_6^-). Examples presented in the context of the organometallic approach are members of the series $[\text{Cr}\{\eta^6\text{-C}_6\text{H}_6 - n(\text{CO}_2\text{H})_n\}(\text{CO})_3]$, where $n = 1-3$.

Introduction

Inorganic crystal engineering implies the involvement of metals in extended assemblies. The purpose of involving metals may be purely structural, *e.g.*, providing linkages or controlling network connectivity. The purpose may also be functional, *e.g.* the introduction of metal-based photophysical or magnetic properties or, in channel structures, perhaps even metal-based reactive sites.

When considering the involvement of transition metals in crystal engineering, one has at one's disposal several decades worth of well established principles in coordination chemistry and organometallic chemistry upon which to build. Specifically, the linking of transition metal-containing molecular building blocks can draw upon these principals both for design and synthesis of the molecular units. The existing knowledge base includes information upon predominant coordination numbers and coordination geometries for a wide variety of transition metal ions, as well as qualitative or quantitative information on the thermodynamic and kinetic stability of many types of metal–ligand bond.¹ Thus, for example platinum(II) almost exclusively adopts a square-planar four-coordinate geometry. As a soft Lewis acid it forms stronger bonds with ligands whose donor atoms are soft Lewis bases. Indeed, the potential use of these principles of coordination chemistry has already been

demonstrated in the construction of (infinite) coordination polymers² and in the assembly of (finite) molecular polygons and polyhedra.³ Similarly, there are guiding principles such as the 18-electron rule that help rationalize the types of organometallic transition metal compounds that can be formed.⁴ Of particular relevance to the present study is the well developed chemistry of $\text{Cr}(\text{CO})_3(\text{arene})$ compounds.⁵

Our aim in this work has been to combine this well established molecular inorganic chemistry with well established aspects of supramolecular organic chemistry. Specifically, derivatives of arenes used as building blocks impart rigidity and well defined directionality in the propagation of supramolecular assemblies. Hydrogen bonds combine the most favorable aspects of directionality and strength among intermolecular interactions; while they are weaker than covalent bonds or even coordinate bonds, they offer greater flexibility and there are well developed principles for fostering mutual recognition by functional groups through hydrogen bonding.⁶ Thus, arenes bearing self-recognizing hydrogen bonding groups such as carboxyl and amide groups can, in principle, be used to construct hydrogen-bonded assemblies with predictable topologies, as illustrated in Scheme 1 for the case of benzene carboxylic acids.⁷ These assemblies are one- or two-dimensional in nature as a result of the planar arene units.

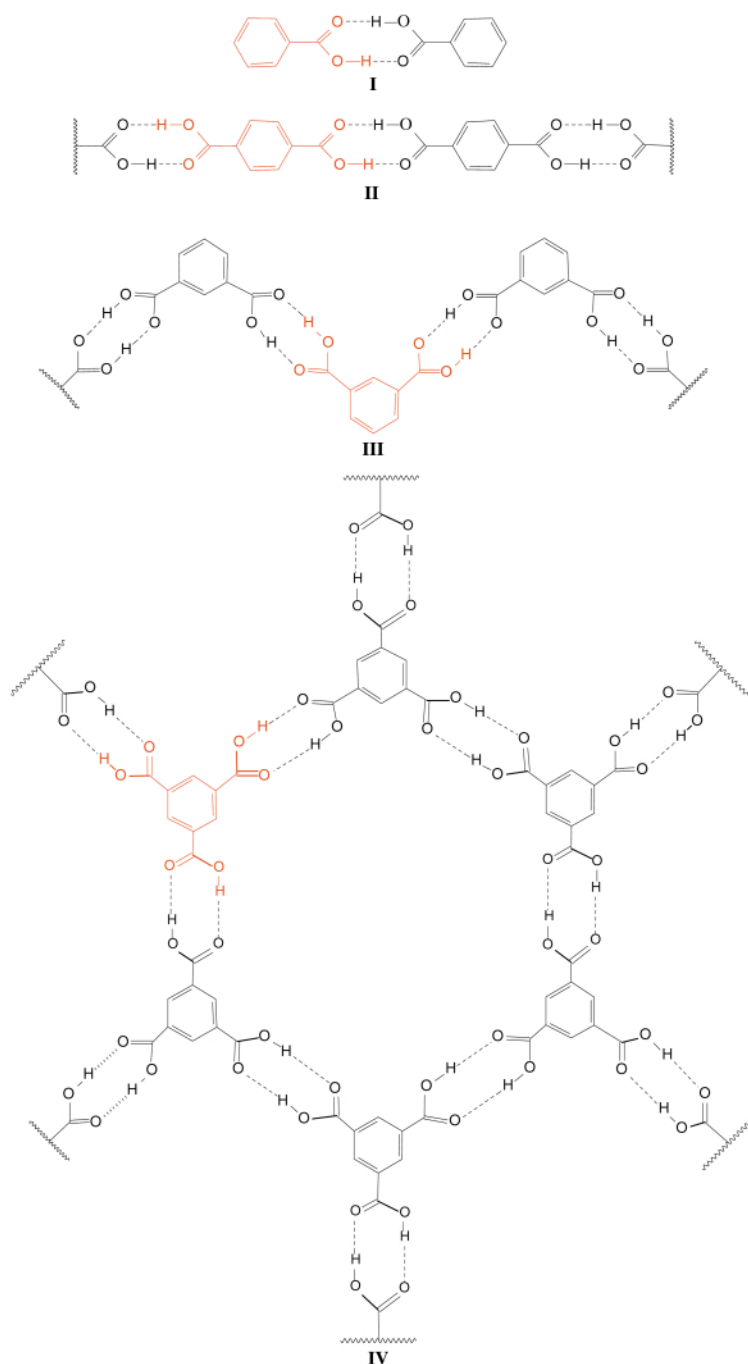
The present work focusses on combining the structural properties of transition metal centers with such arene-based hydrogen bonded networks. This will be accomplished in one of two ways, using coordination chemistry by which the metal center is introduced in the plane of the arene ring(s) and, alternatively, using π -organometallic chemistry in which the metal center is connected orthogonal to the arene plane (Scheme 2). It should be noted here that, depending upon the connectivity utilized at the metal center, the final inorganic assembly may be of equal

† Based on the presentation given at Dalton Discussion No. 3, 9–11th September 2000, University of Bologna, Italy.

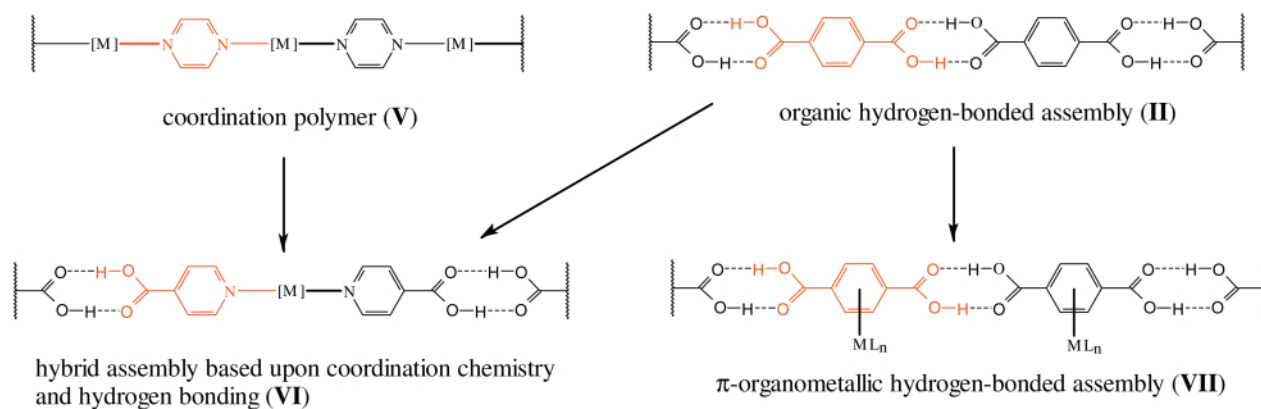
Electronic supplementary information (ESI) available: rotatable 3-D crystal structure diagram in CHIME format. See <http://www.rsc.org/suppdata/dt/b0/b004395h/>

‡ Present address: Department of Chemistry, University of Edinburgh, West Mains Road, Edinburgh, UK EH9 3JJ.

§ Present address: Instituto Venezolano de Investigaciones Científicas, Caracas, Venezuela.



Scheme 1 Hydrogen bonded dimer, linear and zigzag tapes, and 2D honeycomb network established by benzoic acid (**I**), terephthalic acid (**II**), isophthalic acid (**III**) and trimesic acid (**IV**), with molecular building blocks highlighted in red.

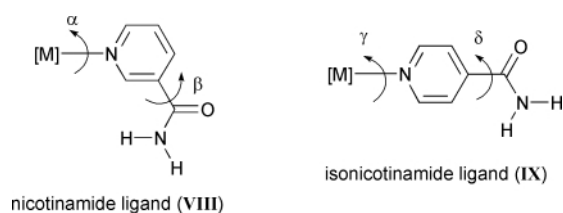


Scheme 2 Illustration of the incorporation of metals into 1D hydrogen bonded-assemblies, *via* coordination chemistry (**VI**) or π -organometallic chemistry (**VII**), and their relationship to the parent organic hydrogen-bonded assemblies (**II**) and coordination polymers (**V**).

of greater dimensionality than the parent (1D or 2D) organic assembly.

Taking the linear hydrogen-bonded assembly observed for terephthalic acid (**II**) as a prototype of organic crystal engineering, one can envision substituting the carboxylic acid dimer linkage by a linear connection comprising coordination of two heterocyclic aromatic ligands to *trans* sites at a transition metal center. Thus, the $R_2^2(8)$ hydrogen-bonded supramolecular synthon⁸ is replaced by a linear N–M–N synthon. Substitution of alternate hydrogen-bonded links yields a hybrid structure (**VI**). Conceptually analogous is the relationship between the coordination polymer (**V**) and the hybrid structure (**VI**), which requires substitution of the N–M–N synthon by a carboxyl dimer at alternate sites along the chain. Obviously **II**, **V** and **VI** are not chemically interconvertible in any simple manner, but the topological or supramolecular relationship between the three structures is clear.¶ Simple linear assemblies analogous to **V** can in principle be achieved using metal centers, [M], that are two-, four-, five- or six-coordinate with the two pyridine-based ligands adopting a mutually *trans* arrangement. That this can be achieved in practice has been demonstrated by the work of Aakeröy *et al.* who have combined silver(I) salts with the bifunctional arene ligands pyridine-4-carboxamide (isonicotinamide) and pyridine-4-aldoxime yielding crystalline materials containing (cationic) linear assemblies similar to **V**.⁹ Coordination of the corresponding carboxylic acid, isonicotinic acid, to Ag^+ results in deprotonation of half of the carboxyl groups to give a related (neutral) assembly in which the hydrogen-bonded link is between a carboxyl and a carboxylate group.¹⁰

Inorganic–organic hybrid assemblies with a wide range of topologies should be accessible by this coordination chemistry/hydrogen bonding approach. Simple variations from the linear assemblies may, in principle, be accomplished by changing the substitution pattern on the arene ring [*cf.* the change in the parent system on going from terephthalic acid (**II**) to isophthalic acid (**III**)] or by changing the stereochemistry at the metal center (*viz.* *cis* coordination of the two ligands rather than *trans*). Further variety can be introduced by connecting more than two of the bifunctional arene ligands to each metal center (*vide supra*). In the present report we will focus on the use of square-planar Pt(II) metal centers in combination with four nicotinamide (**VIII**) or isonicotinamide (**IX**) ligands (Scheme 3).



Scheme 3 Nicotinamide (pyridine-3-carboxamide) and isonicotinamide (pyridine-4-carboxamide) ligands. Curved arrows indicate torsional flexibility at positions α – δ .

Returning now to the terephthalic acid assembly as the organic prototype, an alternative modification that introduces transition metal centers is simply to connect a suitable (12-electron) metal–ligand moiety, ML_n , to the arene by π -coordination. In contrast to the prior strategy using coordination chemistry, none of the original supramolecular synthons need to be replaced by metal-mediated connections. The ML_n moieties can be thought of in the first instance as appendages to the parent organic assembly. One can conceive of this “appendage” being designed so as to provide structural control of the

¶ The carboxyl dimer and N–M–N synthons have dissimilar length scales (ring to ring separation, $C \cdots C$ ca. 6.7–6.9 Å vs. $N \cdots N$ ca. 3.8–4.4 Å).

assembly, such as in the design of channels, or being used to introduce specific metal-centered physical properties. We will describe our efforts to prepare a first generation of organo-metallic assemblies using this approach, specifically by π -coordination to $Cr(CO)_3$ of each of the four benzene carboxylic acid building blocks illustrated in Scheme 1.

In presenting work using these two approaches for the inclusion of transition metals in hydrogen bonded assemblies, we will provide examples, discuss the potential of these approaches and point out some of the pitfalls. The structures of eight compounds will be described, some as solvates. Four are based upon the coordination chemistry approach (compounds **1–4**) and four are based upon the organometallic π -arene approach (compounds **5**, **7**, **9** and **10**). Preliminary reports of some of these examples (**1**, **2**, **5** and **10**) have appeared in previous communications.^{11,12}

Experimental

General procedures

Syntheses of compounds **1–4** were conducted under an inert atmosphere, but such precautions should in fact be unnecessary.¹³ For the syntheses of compounds **5–10**, organic solvents were dried according to standard purification procedures, distilled and degassed prior to use. All manipulations of air- or water-sensitive materials (**5–10**) were carried out using Schlenk-line techniques. NMR spectra were recorded on a Bruker ARX-500, Varian Unity Plus-300 or Varian XL-300 spectrometer. IR data were recorded on either a Perkin-Elmer 1600 Series or Mattson 6200 FT-IR spectrometer. Elemental analyses were conducted by Schwarzkopf Microanalytical Laboratory, Woodside, New York, USA. Crystal yields were not recorded. However, either crystal structure determinations or unit cell determinations were conducted on a number of crystals as a crude test of sample homogeneity.

Syntheses

[Pt(VIII)₄]Cl₂ 1. Compound **1** was prepared in quantitative yields using well established methods¹³ *via* the stoichiometric reaction of $K_2[PtCl_4]$ with nicotinamide (**VIII**) in aqueous solution. The product was formed as a colorless solution, which upon slow cooling and evaporation of solvent yielded colorless crystals that were suitable for X-ray diffraction studies. δ_H (500 MHz, D_2O , 298 K): 7.64 (dd, $J = 8.1, 5.5$ Hz), 8.33 (d, $J = 8.1$ Hz), 9.03 (d, $J = 5.5$ Hz), 9.24 (s). δ_C (125.5 MHz, D_2O , 298 K): 128.20, 133.60, 140.58, 151.75, 154.53, 167.60. IR (KBr, cm^{-1}): 565m, 652m, 761m, 812m, 951w, 1123m, 1162w, 1199m, 1249m, 1390s(br), 1488w, 1578s, 1630s(br), 1687s(br), 1990vw, 2999vs(br), 3148vs(br), 3368vs.

[Pt(VIII)₄](PF₆)₂ 2. Compound **2** was obtained by an anion exchange reaction through addition of a stoichiometric amount of NH_4PF_6 to an aqueous solution of **1**. The colorless solution was slowly evaporated and yielded colorless crystals of **2**· H_2O of sufficient quality to be studied by X-ray diffraction. The 1H and ^{13}C NMR spectra of such crystals dissolved in D_2O were as expected identical to that of **1**. The anion exhibited a ^{31}P NMR signal at δ 0.22.

[Pt(IX)₄]Cl₂ 3. Compound **3** was prepared in quantitative yield from $K_2[PtCl_4]$ and isonicotinamide (**IX**) in aqueous solution following a procedure identical to that used to prepare **1**. Slow evaporation of the colorless solution of the product gave a colorless crystalline material that was characterized spectroscopically by NMR and IR, crystallographically by X-ray diffraction as **3**· $7H_2O$ and by C, H, N elemental analysis. δ_H (500 MHz, D_2O , 298 K): 7.90 (d, $J = 6.7$ Hz), 9.02 (d, $J = 6.7$ Hz). δ_C (125.5 MHz, D_2O , 298 K): 125.95, 145.47, 153.10, 168.13. IR (KBr, cm^{-1}): 644s, 770m, 865m, 951w, 1002w, 1062m, 1123w,

1233m, 1295w, 1396s, 1430(sh), 1551m, 1618s(br), 1685s(br), 1885vw, 1960vw, 2130vw, 2470vw, 3156vs(br), 3318vs(br). (Calc. for 3·8H₂O: C, 32.08; H, 4.45; N, 12.42. Found: C, 32.21; H, 4.56; N, 12.34%).

[Pt(IX)₄](PF₆)₂ 4. Compound **4** was obtained by an anion exchange reaction through addition of a stoichiometric amount of NH₄PF₆ to an aqueous solution of **3**. The colorless solution was slowly evaporated and yielded colorless crystals of sufficient quality to be studied by X-ray diffraction. δ_{H} (500 MHz, D₂O, 298 K): 7.83 (s, br), 8.78 (s, br). δ_{C} (125.5 MHz, D₂O, 298 K): 125.2, 145.1, 152.9, 169.1. IR (KBr, cm⁻¹): 511w, 560s, 630m, 844s(br), 1027w, 1145m, 1240w, 1300m, 1402s, 1553w, 1627s(br), 1685s(br), 3171vs(br).

[Cr(η^6 -PhCO₂H)(CO)₃] 5. Preparation and full spectroscopic characterization of **5** has been reported in an earlier communication.¹² The isolated product contained orange crystals suitable for X-ray diffraction.

[Cr(η^6 -C₆H₄(CO₂Me)₂-1,4)(CO)₃] 6. Compound **6** was prepared using only a minor deviation from the literature procedure.¹⁴ A solution containing dimethylterephthalate, C₆H₄(CO₂Me)₂-1,4 (3.0 g, 15.4 mmol) and Cr(CO)₆ (6.8 g, 30.9 mmol) in deoxygenated di-*n*-butyl ether (155 mL) and THF (10 mL) was refluxed overnight under N₂. Upon cooling, the mixture was filtered through Celite to remove unreacted and oxidized chromium products. After removal of solvents, the resulting orange solid was recrystallized from CH₂Cl₂ and then from diethyl ether. δ_{H} [300 MHz, (CD₃)₂CO, 298 K]: 3.93 (s, 6H), 6.05 (s, 4H); δ_{C} [75.42 MHz, (CD₃)₂CO, 298 K]: 53.3, 91.8, 165.9, 229.4. The crystal structure of **6** has been previously reported.¹⁵

[Cr(η^6 -C₆H₄(CO₂H)₂-1,4)(CO)₃] 7. Compound **7** was prepared by saponification of the ester complex **6**. Thus, to a solution of KOH (150 mg) in THF (50 mL) and deionized water (10 mL) was added 260 mg of **6**. The solution was stirred overnight under N₂. To the resulting yellow solution was added 10 mL deionized water. The THF was removed using a rotary evaporator, and the solution was washed with diethyl ether (2 × 100 mL). The aqueous component containing the organometallic salt K₂[Cr(η^6 -C₆H₄(CO₂)₂-1,4)(CO)₃] was treated with HCl (10%) until a pH of *ca.* 1 was obtained. The product, **7**, was extracted into diethyl ether (2 × 100 mL) and dried using MgSO₄. The solvent was evaporated and the resulting red-orange solid was recrystallized from DMSO–diethyl ether and yielded orange crystals of 7·2DMSO suitable for X-ray diffraction. δ_{H} [300 MHz, (CD₃)₂CO, 298 K]: 6.29 (s); δ_{C} [75.42 MHz, (CD₃)₂CO, 298 K]: 94.3, 94.8, 165.6, 231.4. IR (KBr, cm⁻¹): 1691s (C=O), 1933vs (C=O), 1995s (C=O).

[Cr(η^6 -C₆H₄(CO₂Me)₂-1,3)(CO)₃] 8. Compound **8** was prepared from dimethylisophthalate, C₆H₄(CO₂Me)₂-1,3 and Cr(CO)₆ using the same procedure as for the preparation of **6**. The resulting orange solid was recrystallized from CH₂Cl₂–diethylether yielding crystals with a monoclinic lattice (mp 89–90 °C). Recrystallization of this material from benzene resulted in a triclinic polymorph (mp 84–85 °C), whereas recrystallization from diethyl ether containing 1,4-phenylenediamine resulted in an orthorhombic form (mp 112–113 °C). Crystal structures have been determined but will be reported in detail elsewhere.

[Cr(η^6 -C₆H₄(CO₂H)₂-1,3)(CO)₃] 9. Compound **9** was prepared by saponification of the ester complex **8** using a procedure identical to that for the preparation of acid complex **7** from the ester complex **6**. The solvent was evaporated and the resulting red–orange solid was recrystallized from DMF–diethylether and yielded orange crystals of 9·2DMF suitable for X-ray diffraction. δ_{H} (300 MHz, CDCl₃, 298 K): 5.20 (t), 5.97 (d), 6.50

(s). δ_{C} [75.42 MHz, (CD₃)₂SO, 298 K]: 90.9, 96.8, 97.9, 165.3, 230.1 (Calc.: C, 45.54; H, 4.50; N, 6.25. Found: C, 45.88; H, 4.46; N, 5.99%).

[Cr(η^6 -C₆H₃(CO₂H)₃-1,3,5)(CO)₃] 10. Preparation of **10**, by direct reaction of C₆H₃(CO₂H)₃-1,3,5 with Cr(CO)₆, and full spectroscopic characterization has been reported in an earlier communication.¹² After filtration of the resulting yellow solution of the product to remove unreacted and oxidized chromium products and subsequent concentration of the dibutyl ether solution, orange crystals of 10·Buⁿ₂O were obtained by slow crystallization over several weeks at –20 °C.

X-Ray crystal structure determinations

Crystals were protected from either reaction with air or solvent loss by coating with a thin layer of hydrocarbon oil prior to mounting on a glass fiber and immersion directly in the cold nitrogen stream of the diffractometer. All intensity data were collected using a Bruker (Siemens) SMART CCD platform diffractometer, solved by direct or Patterson methods and refined to convergence against *F*² data [*F*² > –3σ(*F*²)] using the SHELXTL suite of programs.¹⁶ Data were corrected for absorption using empirical methods (SADABS) based upon symmetry-equivalent reflections combined with measurements at different azimuthal angles.¹⁷ Unless otherwise stated, non-hydrogen atoms were refined anisotropically and hydrogen atoms were placed in calculated positions with idealized geometries and refined using a riding model with fixed isotropic displacement parameters. A summary of the crystallographic data can be found in Table 1.

CCDC reference number 186/2098.

See <http://www.rsc.org/suppdata/dt/b0/b004395h/> for crystallographic files in .cif format.

For the structures of **1**, 2·H₂O and 3·7H₂O, amide hydrogens were located directly from the difference maps and refined without positional constraints. For 3·7H₂O, one solvate water molecule is disordered between two (oxygen atom) positions, O(1a) and O(1b), to each of which 50% occupancy was assigned. Solvate water molecule O(3), though not disordered, also has 50% occupancy. Additionally, these water molecules lie on a crystallographic mirror plane. Thus, the asymmetric unit which is populated by 0.25 formula units, contains 1.75 water molecules. Hydrogen atoms for the solvate water molecules were not located from the difference maps and were not added to the model. For **4**, there are two crystallographically different platinum centers. One [Pt(IX)₄]²⁺ cation is located in a general position and the other lies at an inversion center. There are three crystallographically independent PF₆⁻ anions, all of which are substantially disordered. The disorder was modelled by restraining all P–F and all F···F (*cis*) distances, respectively, to have approximately the same values. Two orientations were then refined for each anion, leading to occupancies of 77:23, 65:35 and 58:42%. Anisotropic displacement parameters of atoms within the pyridine rings N(21)–C(26), N(41)–C(46) and N(51)–C(56) were restrained to be similar to their bonded neighbors.

For structures **5**, 7·2DMSO and 10·Buⁿ₂O, carboxyl hydrogens were located from the difference map and then refined using a simple riding model. For the structure of 9·2DMF, the carboxyl hydrogens were placed in idealized positions and then refined using a riding model that allowed torsional freedom of the O–H vector about the C–O bond. Both DMF solvate molecules exhibited disorder. In one case this consisted of positional disorder between the carbonyl oxygen and formyl hydrogen, and was modelled using only the two partial occupancy oxygen positions (70:30%). In the second molecule, a similar disorder (*ca.* 90:10%) was ignored and the major component was included at 100% occupancy with the formyl hydrogen placed in a calculated position. Rotational

Table 1 Data collection, structure solution and refinement parameters for **1**, **2**·H₂O, **3**·7H₂O, **4**, **5**, **7**·2DMSO, **9**·2DMF and **10**·Buⁿ₃O

	1 ^a	2 ·H ₂ O ^a	3 ·7H ₂ O	4	5 ^a	7 ·2DMSO	9 ·2DMF	10 ·Bu ⁿ ₃ O ^a
Color	Colorless	Colorless	Colorless	Colorless	Orange	Orange	Orange	Orange
Crystal size/mm	0.18 × 0.10 × 0.10	0.10 × 0.04 × 0.04	0.20 × 0.05 × 0.05	0.10 × 0.08 × 0.05	0.28 × 0.20 × 0.08	0.40 × 0.08 × 0.05	0.22 × 0.16 × 0.10	0.38 × 0.24 × 0.18
Crystal system	Triclinic	Triclinic	Monoclinic	Monoclinic	Triclinic	Monoclinic	Triclinic	Triclinic
Space group, <i>Z</i>	<i>P</i> 1̄, 1	<i>P</i> 1̄, 1	<i>C</i> 2/ <i>c</i> , 2	<i>P</i> 2 ₁ / <i>c</i> , 6	<i>P</i> 1̄, 2	<i>P</i> 2 ₁ / <i>c</i> , 4	<i>P</i> 1̄, 2	<i>P</i> 1̄, 4
<i>a</i> /Å	8.1500(1)	9.678(3)	12.6582(1)	8.888(3)	7.0349(3)	8.0183(2)	6.5676(1)	11.6029(3)
<i>b</i> /Å	8.7935(1)	10.099(2)	17.2961(2)	32.843(11)	7.2332(3)	21.3486(3)	10.6471(1)	13.0537(2)
<i>c</i> /Å	10.0075(1)	10.321(2)	7.8045(1)	16.711(4)	11.1518(5)	11.8935(1)	15.3866(2)	15.2638(2)
<i>a</i> /°	85.985(1)	69.03(2)	90	90	88.710(1)	90	79.540(1)	87.472(1)
<i>b</i> /°	89.699(1)	65.396(15)	94.430(1)	98.43(2)	81.733(1)	93.521(1)	77.794(1)	75.734(1)
<i>γ</i> /°	70.680(1)	70.32(2)	90	90	63.012(1)	90	82.222(1)	86.752(1)
<i>V</i> /Å ³	675.05(1)	835.3(4)	1703.59(3)	4825.6(24)	499.82(4)	2032.08(6)	1028.85(2)	2235.89(7)
<i>D</i> _x /g cm ⁻³	1.856	2.007	1.689	2.010	1.715	1.498	1.447	1.415
<i>T</i> /K	213(5)	213(5)	203(5)	203(5)	208(5)	208(5)	208(5)	173(5)
<i>μ</i> (Mo-Kα)/mm ⁻¹	5.442	4.416	4.339	4.578	1.145	0.811	0.606	0.564
<i>θ</i> range/°	2.04–29.80	2.21–29.72	2.00–30.20	1.24–23.00	1.85–29.31	1.91–25.00	1.96–27.50	1.81–22.50
Reflections collected	14500	8747	13033	53008	5785	17215	12220	18389
Independent reflections, <i>n</i> <i>R</i> _{int}	3550 (0.069)	4236 (0.069)	2468 (0.059)	6724 (0.197)	2437 (0.038)	3580 (0.162)	4701 (0.050)	5833 (0.125)
Reflections used in refinement	3550	4236	2468	6709	2437	3580	4701	5507
Least square parameters (<i>p</i>)	190	247	110	655	145	244	269	559
Restraints (<i>r</i>)	0	0	0	304	0	0	1	108
<i>R</i> (<i>F</i>), ^b [<i>I</i> > 2.0 <i>σ</i> (<i>I</i>)]	0.0390	0.0634	0.0343	0.0829	0.0449	0.0689	0.0617	0.1101
<i>wR</i> 2(<i>F</i> ²), ^b (all data)	0.0833	0.1237	0.0808	0.2071	0.1158	0.1909	0.1818	0.3001
<i>S</i> (<i>F</i> ²), ^b (all data)	0.979	1.016	1.078	1.164	1.058	1.042	1.033	1.145

^a Previously reported in preliminary communication: ref. 11 for **1** and **2**·H₂O, ref. 12 for **5** and **10**·Buⁿ₃O, ^b *R*(*F*) = $\Sigma(|F_o| - |F_c|)/\Sigma|F_o|$; *wR*2(*F*²) = $[\Sigma w(F_o^2 - F_c^2)^2/\Sigma w F_o^4]^{1/2}$; *S*(*F*²) = $[\Sigma w(F_o^2 - F_c^2)^3/(n - p)]^{1/2}$.

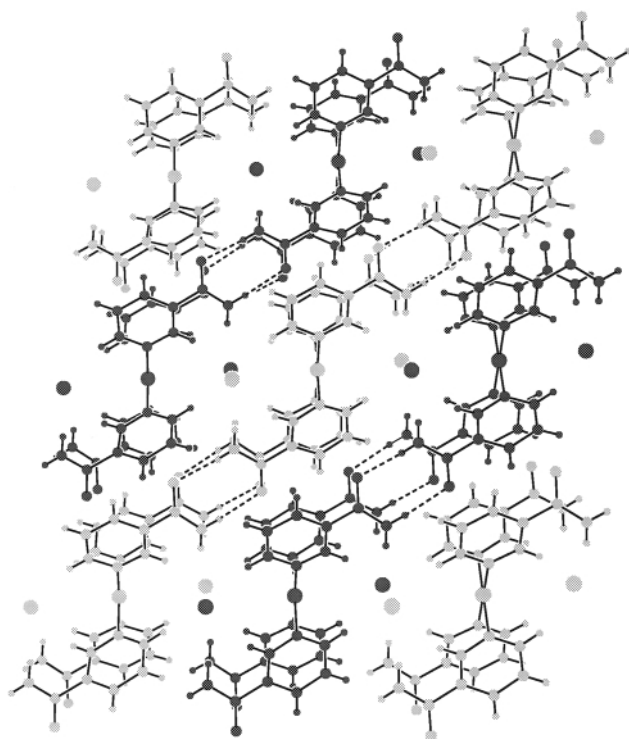


Fig. 1 View of **1** parallel to cation layers shown extending vertically along the *c*-axis (cations shown in alternating grey and black shades). $R_2^2(8)$ amide–amide hydrogen bonding occurs between cations shown with same shading but in different layers and chloride channels run along the *b*-axis perpendicular to the page).

disorder of one of the methyl groups was successfully modelled (73:27%).

Combining coordination chemistry and hydrogen bonds

Four compounds of the general formula $[PtL_4]X_2$ [L = nicotinamide (**VIII**) or isonicotinamide (**IX**); $X^- = Cl^-$ or PF_6^-] have been synthesized and characterized by single-crystal X-ray diffraction as part of our recent efforts to explore the combining of established ideas in coordination chemistry and in hydrogen bonding as a strategy for inorganic crystal engineering. Discussion of the structures will emphasize the supramolecular aspects of these systems, namely the manner in which the (ionic) molecular units assemble to give the overall arrangement in the crystal. The molecular geometries of these systems largely conform to expected norms in terms of bond lengths and angles. Full lists of bond lengths and angles can be found in the Supplementary material (in .cif format). The structures of $[Pt(\text{VIII})_4]Cl_2$ (**1**) and $[Pt(\text{VIII})_4](PF_6)_2 \cdot H_2O$ (**2**· H_2O) have been reported in an earlier communication,¹¹ but are described here to facilitate comparison with $[Pt(\text{IX})_4]Cl_2 \cdot 7H_2O$ (**3**· $7H_2O$), $[Pt(\text{IX})_4](PF_6)_2$ (**4**) and other related systems.

In the structures of **1** and **2**· H_2O the platinum atoms lie at crystallographic inversion centers. The nicotinamide ligands are arranged in a square-planar coordination geometry around the platinum centers. The pyridine rings of the four ligands are oriented approximately perpendicular to the PtN_4 coordination plane of the cation (96.3 and 106.5° in **1**; 98.7 and 96.5° in **2**· H_2O) and such that two amide groups from ligands that lie *cis* to each other are situated on one side of the PtN_4 plane, with the other pair on the other side of the PtN_4 plane. In **1**, all amide groups are involved in $R_2^2(8)$ amide–amide hydrogen-bonded linkages leading to infinite chains of consisting of the cations, shown as molecules of same shading in Fig. 1. At least as important is the fact that the pyridine rings of neighboring molecules associate into a layer structure *via* interdigitation

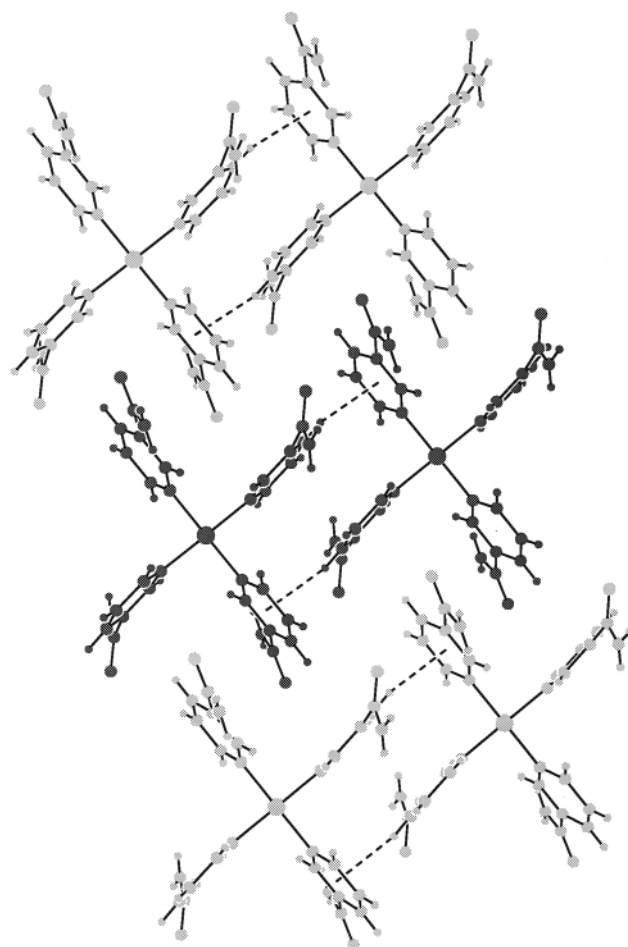


Fig. 2 Single layer of cations of **1** viewed perpendicular to the layer and illustrating the two types of interdigitation between cations (represented in the same shade) along the *b*-axis and between cations (shown in different shades of grey/black) along the *c*-axis. (C–H··· π hydrogen bonds: H··· π 2.55 Å, C–H··· π 160.3°).

involving C–H··· π hydrogen bonds (Fig. 2). Surprisingly, it is this layer structure that is preserved when the same cations are situated in the structure of **2**· H_2O . There is some slippage of the cations within the layer in **2**· H_2O relative to **1** (compare Figs. 3 and 2) that preserves one intralayer cell dimension [$c = 10.0075(1)$ Å in **1** vs. $b = 10.099(2)$ Å in **2**· H_2O] and increases the other [$b = 8.7935(1)$ Å in **1** increases to $c = 10.321(2)$ in **2**· H_2O]. The chloride anions are accommodated in a remarkable channel structure in **1**, and lie at 4.1 Å separations along the *b*-axis.¹⁸ Indeed one might argue that the anions have had a templating effect as they are surrounded by hydrogen bonds from amide N–H and *ortho* C–H groups of the pyridine rings. Thus, all N–H and most C–H groups form structurally important hydrogen bonds in **1**. The PF_6^- anions in **2**· H_2O are too large to be accommodated in the chloride channels and consequently the cation interlayer separation is increased to the extent that the $R_2^2(8)$ amide–amide hydrogen bonds between layers are now absent (Fig. 4). This is also reflected in the increase of the remaining cell dimension from $a = 8.1500(1)$ Å in **1** to $a = 9.678(3)$ Å in **2**· H_2O . The only remaining amide–amide N–H···O hydrogen bonding is now an intralayer [C(12)] arrangement supported by a C(10) chain involving C–H···O hydrogen bonds from the *para* C–H group (Fig. 3). A solvate water molecule occupies a site similar to that of the chloride anions in **1**, *i.e.* approximately axially disposed relative to the platinum centers. Of course, the water molecule can both accept and donate hydrogen bonds in contrast to the chloride ion, which can only serve as an acceptor.

Significantly, when one examines the orientation of the amide groups relative to the pyridine rings (Scheme 3, site β), in

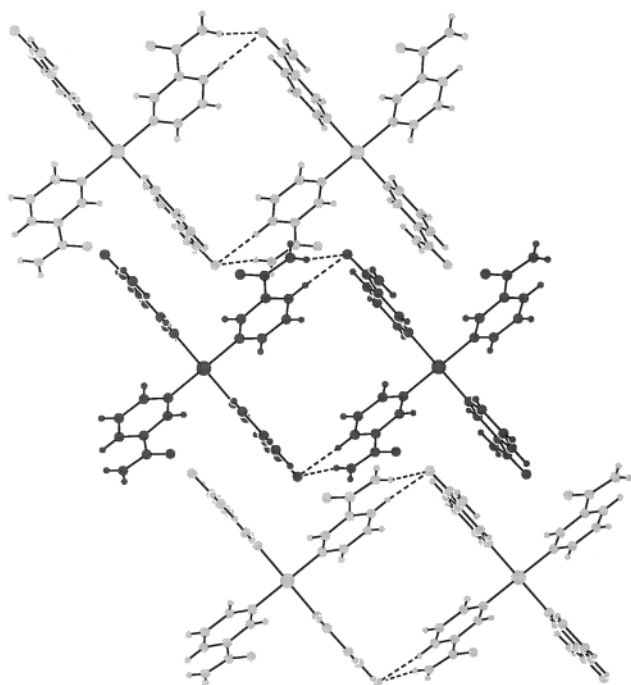


Fig. 3 Single layer of cations of $2\cdot\text{H}_2\text{O}$ viewed perpendicular to the layer, showing interdigitation between cations (represented in different shades) along the b -axis and amide–amide hydrogen bonding between cations (represented in the same shade) along the c -axis.

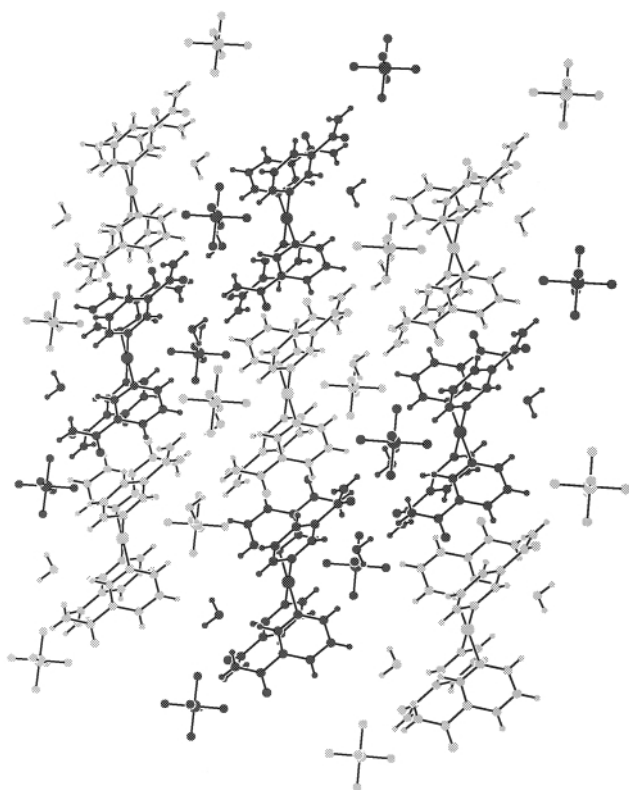


Fig. 4 View of $2\cdot\text{H}_2\text{O}$ parallel to cation layers extending horizontally along the b -axis (neighboring cations are shown in different shades). Anion/solvate layers alternate with the cation layers along the a -axis.

1 the amide groups are slightly twisted away from the conformation in the ring plane ($\text{C}-\text{C}-\text{C}-\text{O}$ torsion angle = 0° shown in Scheme 3) by 20.6 and 31.1° , whereas in $2\cdot\text{H}_2\text{O}$ the amide substituents are oriented closer to the ring plane, with torsion angle of 2.2 and -170.6° . Note that one pair of *trans* related ligands in $2\cdot\text{H}_2\text{O}$ thus has its amide groups rotated by *ca.* 180° relative to the other pair. These arrangements allow the water molecules to accept an $\text{N}-\text{H}\cdots\text{O}$ hydrogen bond and donate an

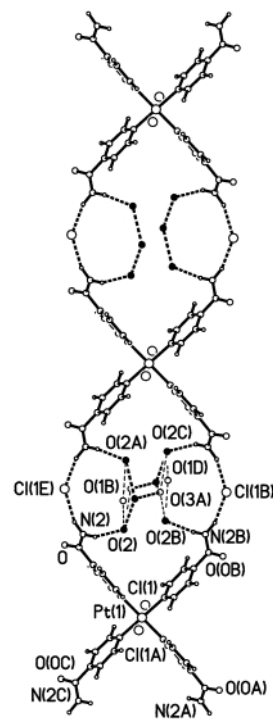


Fig. 5 Linear tape formed by $3\cdot 7\text{H}_2\text{O}$, shown with labelling of key atoms. All sites of disordered water network shown only in lower part. $\text{N}-\text{H}\cdots\text{Cl}$ and shorter $\text{O}-\text{H}\cdots\text{O}$ hydrogen bonds ($\text{O}\cdots\text{O}$ *ca.* 2.6 – 2.7 Å) are shown with thick dashed lines, whereas longer $\text{O}-\text{H}\cdots\text{O}$ hydrogen bonds ($\text{O}\cdots\text{O}$ *ca.* 2.9 – 3.0 Å) are shown with thin dashed lines.

$\text{O}-\text{H}\cdots\text{O}$ hydrogen bond, in contrast to the chloride anions in **1**, which must interact with the amide groups through accepting $\text{N}-\text{H}\cdots\text{Cl}$ hydrogen bonds. The PF_6^- anions in $2\cdot\text{H}_2\text{O}$ accept an $\text{O}-\text{H}\cdots\text{F}$, an $\text{N}-\text{H}\cdots\text{F}$ and a number of $\text{C}-\text{H}\cdots\text{F}$ hydrogen bonds.

On a further note, we were also able to crystallize a polymorph of $2\cdot\text{H}_2\text{O}$ in which all four amide groups lie on the same side of the PtN_4 coordination plane.¹⁹ The overall structure might best be described as a cation bilayer arrangement with water molecules contained within the bilayer and anions forming layers that alternate with the cation bilayer. Unfortunately, to date all data sets exhibit unresolved twinning and have space group ambiguity preventing satisfactory refinement. Nevertheless, this is an important observation as it is indicative of the difficulty in predicting the overall structural arrangement.

Aakeröy and Beatty have reported use of the same ligand ($L = \text{nicotinamide}$) in the structures of $[\text{AgL}_2]\text{X}$ ($\text{X}^- = \text{CF}_3\text{SO}_3^-$, BF_4^- , PF_6^-).^{9a} In these systems all the cations are linked *via* amide–amide hydrogen bonding, though the exact nature of this linkage varies with the anion present. However, despite this variability it is encouraging that there are clearly some persistent structural features, such as the 2D hydrogen-bonded cation sheets observed for both $[\text{AgL}_2]\text{BF}_4$ and $[\text{AgL}_2]\text{PF}_6$.

In comparison to **1** and $2\cdot\text{H}_2\text{O}$, the structures of $[\text{Pt}(\text{IX})_4]\text{Cl}_2\cdot 7\text{H}_2\text{O}$ ($3\cdot 7\text{H}_2\text{O}$) and $[\text{Pt}(\text{IX})_4](\text{PF}_6)_2$ (**4**) allow us to explore the effect on the overall supramolecular assembly of changing the location of the amide group on the pyridine ring from the 3-position to the 4-position (*i.e.*, **IX** vs. **VIII**). The same anions are used, although different levels of hydration are observed in the structures that we report here. The structure of $3\cdot 7\text{H}_2\text{O}$ is related to that of **1** inasmuch as the chloride ligands are situated axially²⁰ with respect to the coordination sphere of each platinum atom and the cations are linked by hydrogen bonding that connects the amide groups of two *cis* ligands to a similar pair on a neighboring cation. However, the amide groups in $3\cdot 7\text{H}_2\text{O}$ are not linked directly but rather bridged by chloride ions and a disordered network of hydrogen-bonded water molecules (Fig. 5). The disorder is such that in any given arrangement there are

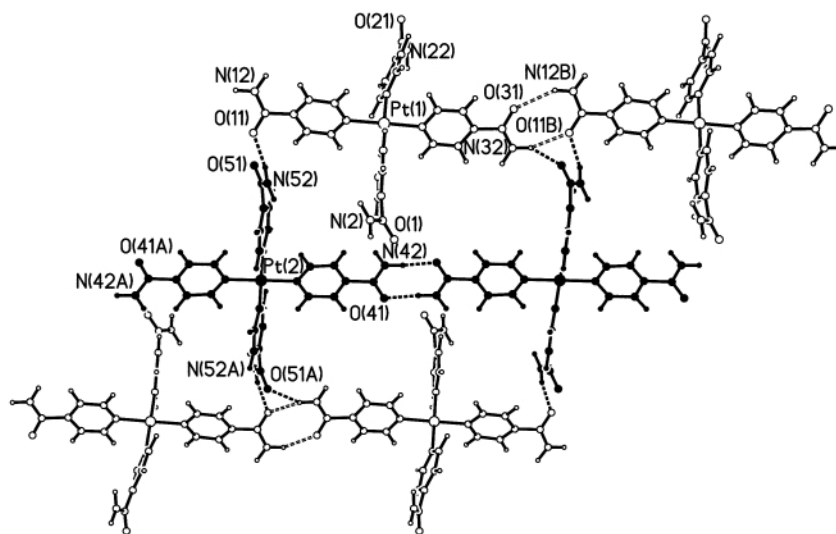


Fig. 6 Structure of **4** showing amide–amide hydrogen bonding propagating tapes along the *c*-axis; type **B** cations are shaded.

seven water molecules present,²¹ the four symmetry-related outer molecules [O(2)] that accept an N–H···O hydrogen bond from the amide groups and three of the six sites that provide the link between the outer water molecules. Thus, the cations are arranged through these hydrogen-bonded links into parallel linear tapes that lie along the *b*-axis. Adjacent tapes are linked *via* hydrogen bonds involving the amide oxygen atoms, which accept O–H···O hydrogen bonds from the water network and C–H···O hydrogen bonds from neighboring cations. Pyridine rings are oriented at 79.4° to the PtN₄ plane, while amide groups are twisted 34.0° out of the pyridine ring plane. Note also that there is only one unique chloride site, indeed one-quarter of the formula unit is crystallographically unique. Thus, each chloride ion that bridges between amide groups also sits in an axial site at a platinum center (Pt···Cl 3.85 Å) from an adjacent tape.

In efforts to further explore the potential utility of the structural arrangement presented in **3**·7H₂O, attempts were made to replace the seven water molecules by a guest molecule that might occupy a similar total volume and also provide hydrogen bond donor and acceptor sites. Recrystallization from an aqueous solution containing glucose yielded crystals with almost identical cell dimensions to that of **3**·7H₂O, but a new pattern of electron density peaks in the region previously occupied by the water molecules in **3**·7H₂O. Efforts to model this region in terms of either a disordered glucose molecule or a new hydration arrangement have to date been unsuccessful.

The structure of **4** contains two independent cations, **A** [Pt(1) site] and **B** [Pt(2) site], present in a 2:1 ratio, and three independent anions. Linear chains, consisting either wholly of type **A** or of type **B** cations propagate along the *c*-axis and lie parallel to one another in a repeating **ABAABA** arrangement along the direction of the *a*-axis (Fig. 6). Within each chain the cations are arranged in a very similar manner. However, while type **B** cations are connected by the familiar R₂²(8) amide dimer arrangement of hydrogen bonds (H···O 1.95 Å, N–H···O 166°), this is not strictly so for type **A** cations. Type **A** cations are slightly rotated so as to raise and lower alternate amide groups along the chain [N(12), O(11) and N(32), O(31)] away from the optimum R₂²(8) dimer interaction (H···O 2.68 Å, N–H···O 127° and H···O 2.53 Å, N–H···O 132°). These amide groups are, however, bridged by hydrogen bonding to a third amide group [N(52), O(51)] from the neighboring chain of type **B** cations (H···O 1.95 Å, N–H···O 153° and H···O 2.37 Å, N–H···O 145°). The remaining amide groups on the type **A** cations [N(2), O(1) and N(22), O(21)] provide hydrogen-

bonded links between the type **A** chains. The overall arrangement leads to channels parallel to the *b*-axis that are occupied by the PF₆[−] anions (Fig. 7).

Of particular relevance to this work is a recent paper in which Aakeröy *et al.* suggest that channel structures of this type, *i.e.* [PtL₄]X₂, may have future potential for host–guest chemistry.²² Perhaps this is the case. Indeed it is interesting that there are some similarities between the cation grid arrangement in **4** and that in the structure of **3**·4L (L = isonicotinamide), which was crystallized from a water–ethanol solution of (NH₄)₂[PtCl₄] and isonicotinamide (1:5) after removal of the initial product,²² presumably [PtL₂Cl₂]. In **3**·4L the channels are occupied by additional isonicotinamide ligands rather than by PF₆[−] anions as in **4**. In fact **3**·4L shares some of the features of both **3**·7H₂O and **4**, since cations are linked in one direction *via* amide–amide hydrogen bonds [R₂²(8) arrangement] as in **4** and in the perpendicular direction *via* N–H···Cl hydrogen bonds as in **3**·7H₂O. By contrast, the structure *trans*-[NiL₄(OH₂)₂]ClO₄·2H₂O (L = isonicotinamide), which also has the four isonicotinamide ligands in a square-planar arrangement, forms a cation sheet structure *via* catemer-type amide–amide N–H···O hydrogen bonds.²² This is quite different from **3**·7H₂O, **3**·4L and **4**, but again provides small channels containing the ClO₄[−] counterions.

Overall these structures illustrate the potential of combining coordination chemistry and hydrogen bonding with a view to designing and controlling new crystalline materials. Coordination chemistry is able to provide excellent predictability in ligand arrangement that can be used to direct hydrogen bonding groups *via* rigid ligands bearing suitable substituents. Furthermore it offers a variety of metal centers with reliably achieved coordination geometries, ranging from linear through square-planar and tetrahedral to octahedral. Hydrogen bonding arrangements exhibit a degree of predictability,^{6c} but their inherent weakness leaves open the possibilities of different arrangements of similar energy. Despite this fact, robust hydrogen-bonded organic materials have been prepared,²³ so the potential of this combined approach is clearly there.

On the down side, the influence of choice of anion, and the possible incorporation of solvent molecules, both of which are often more than “space fillers” and typically can participate in hydrogen bonding, is a critical issue to deal with in controlling the assembly of the present systems that comprise cationic metal complexes as building blocks. An illustration of this problem^{10b} is obtained by considering the twenty crystal structures presently in the Cambridge Structural Database that con-

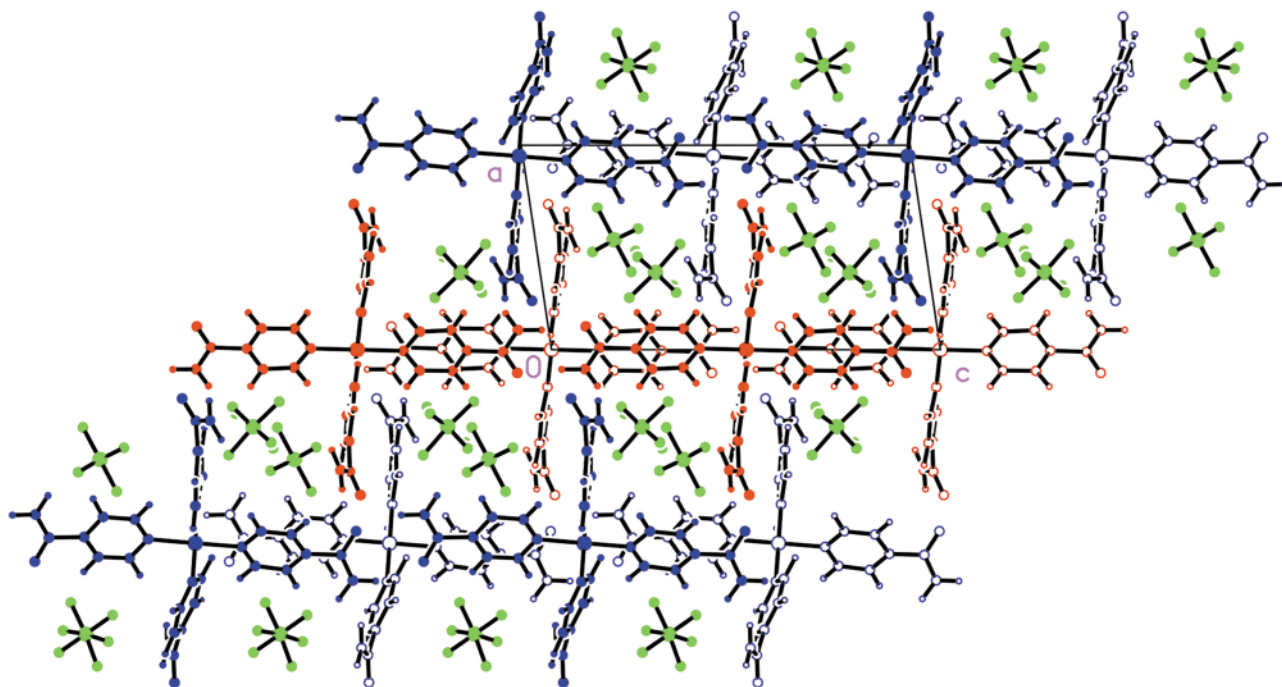


Fig. 7 Structure of **4** showing square grid structure of cations and anion channels along the *b*-axis (parallel to viewing direction). Hydrogen bonds are not explicitly indicated; type **A** cations are in blue, type **B** cations are in red. Cations represented as open circles lie below those that are shaded.

tain at least one isonicotinic acid (**7**) or isonicotinamide (**13**) ligand.²⁴ Of these, only one involves a carboxyl–carboxyl hydrogen bonded dimer,^{24a} two involve infinite chains propagated *via* carboxyl–carboxylate hydrogen bonds^{10a,22} and four involve no interaction between carboxyl groups.^{24b} Among the isonicotinamide-containing systems, only two systems contains the $R_2^2(8)$ hydrogen bonded arrangement,^{22,24c,d} five systems adopt $N-H\cdots O$ hydrogen bonded catemer arrangements,^{24f} and six show no direct interaction between amide groups.^{24g}

However, perhaps some potential problems can ultimately be turned to advantage, say by incorporating the anions as part of the design of a hydrogen-bonded network strengthened by cation–anion interactions. Alternatively, these potential problems can perhaps be avoided by using anionic ligands to produce neutral building molecular blocks and by applying crystallization conditions designed to thwart solvent inclusion. Indeed, Mingos, Burrows and co-workers, in a related approach have accomplished some of these objectives. They have prepared robust metal-containing hydrogen-bonded networks by designing anionic ligands that bind strongly to metals in a chelating manner and can form multiple (often triple) hydrogen bonds to neighboring molecules.²⁵ Burrows and co-workers have also employed anions capable of forming complementary with the cationic metal complexes in such chelate–ligand systems.^{25c,d} In other pertinent work, Hubberstey and co-workers have reported copper coordination compounds that utilize the ligand, 2-cyanoguanidine, that is monodentate in its metal binding, but capable of multipoint hydrogen bonding.²⁶ Puddephatt and Muir have also reported use of pyridine-3,5-dicarboxylic acids in square-planar Pd(II) building blocks.²⁷

At this stage, there are insufficient closely related structures based upon the approach described here of combining coordination chemistry with hydrogen bonding to draw any broad conclusions as to future success. Nevertheless, at the very least it is clear that in most instances, where the intent has been to directly link metal complexes through hydrogen bonding then hydrogen bonding linkages are realized. It is also apparent already that when chemically similar building blocks are used, similarities in connections between building blocks and even overall networks may be observed. This is promising with regards to ultimately gaining some genuine control over the assembly process and being able to design useful new materials.

Combining organometallic π -arene chemistry and hydrogen bonds

In this section we will discuss the structures of four compounds that have been prepared to illustrate the idea of appending a transition metal-containing component to an organic supramolecular assembly that is propagated *via* hydrogen bonds. Specifically our approach has been to prepare a series of compounds by η^6 -coordination to a $Cr(CO)_3$ moiety of arene rings bearing carboxyl substituents [$C_6H_{6-n}(CO_2H)_n$] that are known to form extended networks ($n \geq 2$) in the solid state structures of the parent arenes. It should be noted at this point that there are a few examples in the literature of compounds prepared for other reasons, which are consistent with this approach. In particular, see the observations on the relationship between the crystal structures of [$Fe(\eta^2-(E)-HO_2CCH=CHCO_2H)(CO)_4$], [$Fe(\eta^2-(Z)-HO_2CCH=CHCO_2H)(CO)_4$] and those of the parent organic acids.²⁸

Specifically discussed here will be [$Cr(\eta^6-PhCO_2H)(CO)_3$] (**5**), [$Cr\{\eta^6-C_6H_4(CO_2H)_2-1,4\}(CO)_3\} \cdot 2DMSO$ (**7**·2DMSO), [$Cr\{\eta^6-C_6H_4(CO_2H)_2-1,3\}(CO)_3\} \cdot 2DMF$ (**9**·2DMF) and [$Cr\{\eta^6-C_6H_3(CO_2H)_3-1,3,5\}(CO)_3\} \cdot Bu^n_2O$ (**10**· Bu^n_2O). A preliminary report of the structures of **5** and **10**· Bu^n_2O has appeared in an earlier communication.¹² As in the previous section the emphasis in presentation and discussion of the results will be upon the supramolecular rather than intramolecular aspects of the structures. A full listing of bond lengths and angles can however be found in the Supplementary material (in .cif format).

The structure of **5** contains dimers linked *via* the $R_2^2(8)$ hydrogen-bonding synthon (Fig. 8), well known as a recognition motif between carboxyl groups, and thus resembles the structure of the parent benzoic acid.^{7a} Related carboxamide structures [$Cr(\eta^6-PhCONH_2)(CO)_3$] and [$Cr(\eta^6-PhCH_2CONH_2)(CO)_3$] also exhibit the same manner of molecular recognition.²⁹ It is important to note that the dimer in **5** is centrosymmetric. Thus, the $Cr(CO)_3$ moieties lie on *opposite* sides of the plane of the two arenes. This will be of increasing relevance with regard to extended assemblies that are accessible when additional carboxyl substituents are present (*vide infra*). These centrosymmetric dimers are stacked as illustrated in Fig. 8(a), but perhaps more interestingly they are assembled into a sheet structure by a number of $C-H\cdots O$ hydrogen bonds.

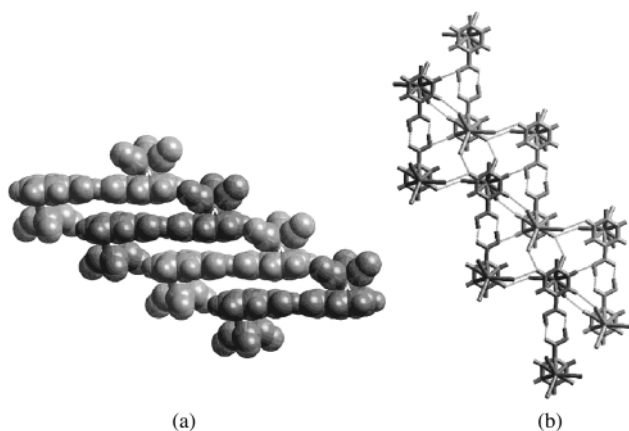
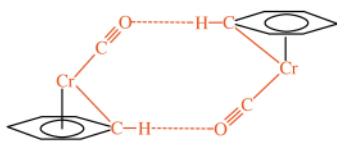


Fig. 8 (a) View of **5** showing stacking arrangement of hydrogen-bonded dimers: (b) View of **5** showing C–H···O hydrogen bonding that links the O–H···O hydrogen-bonded dimers.

Specifically all three carbonyl oxygens serve as hydrogen bond acceptors to C–H donors in the 2- and 5-positions on the arene ring (the latter is a bifurcated donor) linking neighboring molecules *via* $R_2^2(10)$ motifs [Scheme 4, Fig. 8(b)]. Additionally, the



Scheme 4 $R_2^2(10)$ hydrogen bonded linkage observed in **5** [see Fig. 8(b)].

C–H group in the 3-position on the ring forms a C–H···O hydrogen bond to a neighboring hydroxy oxygen. While **5** may be thought of as a “zero dimensional” assembly when one focusses only on the strong O–H···O hydrogen bonds between carboxyl moieties, it clearly illustrates the important role of C–H···O hydrogen bonds in the defining overall arrangement in these organometallic assemblies. The importance of C–H···O hydrogen bonds has been demonstrated in the broader context of organometallic crystal engineering in work by Braga, Grepioni, Desiraju and co-workers,³⁰ and has been an important aspect of our own prior work on hydrogen-bonded salts, $R_3NH^+Co(CO)_4^-$.³¹

Turning now to the structures in which the building blocks contain more than one carboxyl substituent on the arene ring, it

is apparent from reports of the structures of the parent organic acids that these compounds are very difficult to crystallize in the absence of lattice solvent molecules.⁷ The problem lies in crystallization from solution, wherein the target compounds can typically only be dissolved in solvents that also exhibit potent capability to form hydrogen bonds. The problems are not diminished with compounds **7**, **9** and **10**. Thus, here we report crystal structures of the solvates **7**·2DMSO, **9**·2DMF and **10**·Buⁿ₂O.

Hydrogen bonded tape formation analogous to that seen for terephthalic acid (**II**) is prevented in **7**·2DMSO by interaction of DMSO molecules with each of the carboxyl groups. DMSO serves as a strong hydrogen bond acceptor (here O–H···O) but also contributes weaker C–H···O hydrogen bonds involving the carbonyl groups. Perhaps the most interesting feature is again the arrangement of these **7**·2DMSO units into tapes containing coplanar arene rings linked *via* quadruple C–H···O hydrogen bonds (DDAA···AADD)³² that occupy *all* arene C–H groups (Fig. 9). Thus, the DMSO solvent molecule extends the terephthalic acid unit and provides an additional oxygen site that can accept C–H···O hydrogen bonds. Within these tapes all Cr(CO)₃ moieties lie on the *same* side of the arene planes. Adjacent tapes adopt an antiparallel arrangement related by the 2₁-axis parallel to *b* (Fig. 10) and are linked by further C–H···O hydrogen bonds involving the DMSO methyl groups and both the carboxyl groups and carbonyl ligands as acceptors. There is even the suggestion of the presence of a chain of weak C–H···S hydrogen bonds between DMSO molecules (H···S 2.99 Å, C–H···S 136°).

The DMF solvent molecules adhere to the carboxyl groups of the isophthalic acid moiety in the crystal structure of **9**·2DMF in a manner very similar to that just described for DMSO and **7**. Thus, again there are no hydrogen bonds between carboxyl groups and we can consider the entity **9**·2DMF as the building block of the structure. Once more it is C–H···O hydrogen bonds that link these V-shaped building blocks into tapes (ADDAA···DAAAD pattern³² including two bifurcated interactions, Fig. 11). Again all Cr(CO)₃ moieties lie on the *same* side of the tape. Only two of the four arene C–H groups form hydrogen bonds. The two remaining arene hydrogens, H(2) and H(5), are involved in a remarkably short repulsive contact (H···H separation 1.945 Å, *cf.* 2.40 Å for a van der Waals contact³³) that results in some puckering of the tape.

The trimesic acid derivative, **10**, was also crystallized as a solvate **10**·Buⁿ₂O. The dibutyl ether solvent molecule occupies one of the three carboxyl groups though accepting an

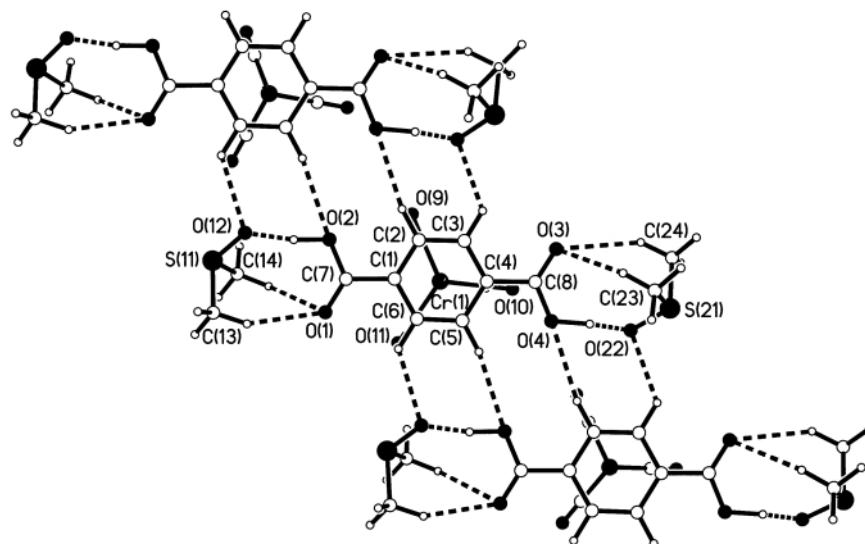


Fig. 9 Structure of **7**·2DMSO with atomic labelling showing hydrogen bonding between carboxyl groups and DMSO molecules and quadruple C–H···O hydrogen bonds (DDAA···AADD) linking **7**·2DMSO units into tapes (chromium, sulfur and oxygen atoms are shaded).

O–H···O hydrogen bond. This leaves the remaining two carboxyl groups to link to neighboring molecules *via* a familiar $R_2^2(8)$ arrangement of O–H···O hydrogen bonds. Thus, the organometallic species, **10**, forms a zigzag ribbon (Fig. 12) reminiscent of the structure of isophthalic acid (**II**) and its derivatives,^{7d,e,34} an arrangement not frequently observed for the parent trimesic acid.³⁵ As in the structures of **7**·2DMSO and **9**·2DMF, the Cr(CO)₃ moieties lie on the *same* side of the ribbon. Solvent channels containing the anchored dibutyl ether molecules now segregate the organometallic ribbons. Carboxyl and carbonyl oxygens also serve as acceptors of a number of C–H···O hydrogen bonds.

Overall, this series of organometallic structures suggests that the approach outlined at the outset has promise but much more work yet needs to be done. Firstly, the desired compounds were successfully synthesized, although the stability of the metal–arene bond decreases as the number of (electron-withdrawing) carboxyl substituents increases. In solution, arene ligand loss is a common mode of decomposition of the organometallic molecules. Only two of the four compounds were obtained in a crystalline form in which the organometallic molecules were linked *via* direct interaction between carboxyl groups in a manner resembling known behavior of the parent organic acid. The problem of obtaining crystals of these compounds in

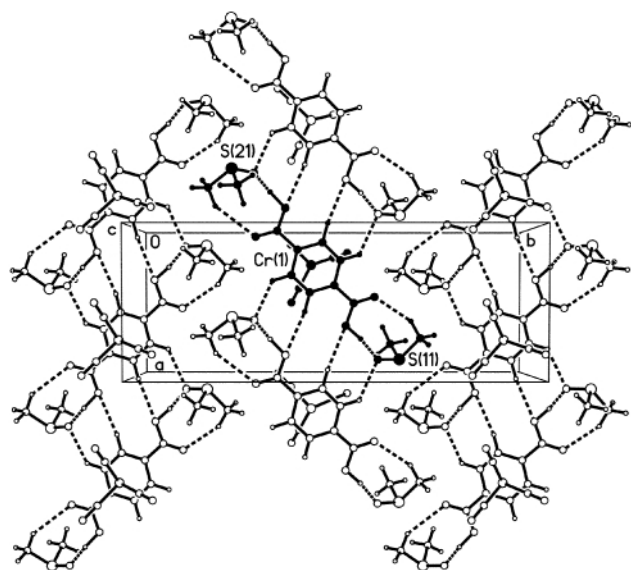


Fig. 10 Antiparallel relationship between adjacent tapes in **7**·2DMSO. One **7**·2DMSO unit is shaded to emphasize the fact that this unit is the building block for the structure. Hydrogen bonds between the three tapes are not shown for reasons of overall clarity.

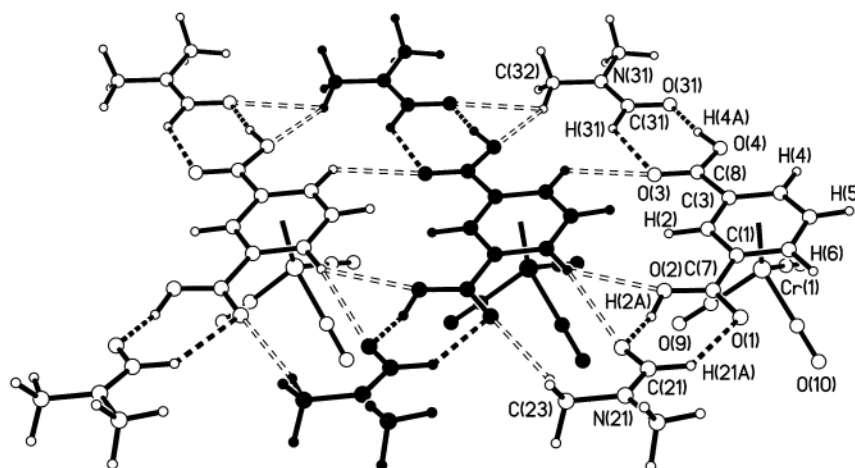


Fig. 11 Puckered tape in which **9**·2DMF units are linked by C–H···O hydrogen bonds. One **9**·2DMF unit is shaded to emphasize the fact that this unit is the building block for the structure. Puckering occurs due to repulsion between H(2) and H(5) arene hydrogens (H···H 1.945 Å, C–H···H 137.6, 140.1°).

the absence of a strongly hydrogen-bonding solvent that can disrupt the carboxyl–carboxyl interactions needs to be overcome. All four structures remind us of the importance of (weaker) C–H···O hydrogen bonds³⁶ in organometallic systems such as these. Indeed, such hydrogen bonds are the primary means of propagating the molecular building blocks into extended structures for **5**, **7**·2DMSO and **9**·2DMF. Solvent molecules DMSO and DMF are very effective at blocking the carboxyl sites, but interestingly provide an extended trimolecular building block in both **7**·2DMSO and **9**·2DMF that is then propagated into a supramolecular tapes *via* C–H···O hydrogen bonds.

The goals in selecting organometallic building blocks that are reasonably straightforward to synthesize in order to test the general approach have effectively been met. Our present efforts in this area are aimed at designing a new generation of improved, more effective organometallic building blocks. Changes that are being explored include: (i) use of ML_n moieties other than Cr(CO)₃; (ii) improving the coordinating ability of the arene ligands; (iii) use of hydrogen bonding groups other than carboxyl; (iv) use of cyclopentadienyl-based systems rather than arenes.

Conclusions and future potential

The work described demonstrates the potential and the difficulties of incorporating transition metals into hydrogen-bonded assemblies by a coordination chemistry route and an organometallic chemistry route. Transition metals have the potential to play either a structural role or a functional role (*i.e.* imparting physical or chemical properties) in this area of inorganic crystal engineering. We have used platinum(II) centers in the coordination chemistry approach to provide a square-planar environment and have used the Cr(CO)₃ moiety to which to bind the arene in the organometallic approach. Each has been combined with fairly simple organic components that provide the hydrogen bonding capability in the resulting inorganic–organic hybrid systems. These systems have provided some success and some failures, at least in terms of preconceived notions of the assemblies that may form through self-complementary hydrogen bonding, but even “failures” can turn up interesting observations (*viz.* C–H···O hydrogen bonding) or suggest ways to improve the design, as is the case here. There is scope to incorporate a wide variety of metals into hydrogen-bonded assemblies by these two approaches. There is also much still to learn prior to achieving a satisfactory level of predictability of the final arrangement of molecules. A systematic approach is needed in which the effect of small structural and electronic changes in the building blocks upon the final assembly is

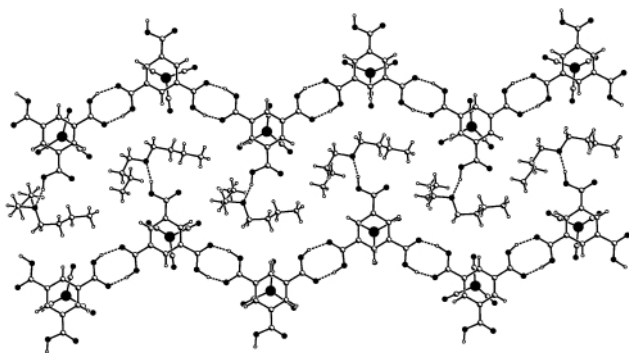


Fig. 12 Structure of $10 \cdot \text{Bu}^3\text{O}$ depicting the hydrogen-bonded zigzag ribbons of **10** and the solvent channels in which Bu^3O solvent molecules are anchored via an $\text{O}-\text{H} \cdots \text{O}$ hydrogen bond as well as a number of $\text{C}-\text{H} \cdots \text{O}$ hydrogen bonds (not shown); chromium and oxygen atoms are shaded.

assessed. As noted above, we are pursuing such a strategy to further develop these approaches.

Acknowledgements

This work was funded in part by the Donors of the Petroleum Research Fund, administered by the American Chemical Society, and by grants from the Missouri Research Board and the University of Missouri-St. Louis. JCMR acknowledges further support in the form of fellowships from the UMSL graduate school and Mallinckrodt Chemical Co. R. A. is grateful for support from the Instituto Venezolano de Investigaciones Científicas and CONICIT. The Bruker ARX-500 NMR spectrometer was purchased with support from the U.S. Department of Energy, grant no. DE-FG02-92CH10499. Purchase of the Varian Unity Plus-300 NMR spectrometer and the Bruker (Siemens) SMART diffractometer were funded by NSF grants CHE-9318696 and CHE-9309690, respectively.

References

- 1 F. A. Cotton, G. Wilkinson, C. A. Murillo and M. Bochman, *Advanced Inorganic Chemistry*, Wiley, New York, 6th edn., 1999; M. Gerloch and E. C. Constable, *Transition Metal Chemistry*, VCH, Weinheim, 1994.
- 2 For example, see: R. Robson, in *Comprehensive Supramolecular Chemistry*, Series ed. J.-M. Lehn, Volume eds. J. L. Atwood, J. E. D. Davies, D. D. MacNicol and F. Vögtle, Pergamon, Oxford, 1996, Vol. 6, pp. 733–755; M. J. Zaworotko, *Chem. Soc. Rev.*, 1994, **23**, 283; K. A. Hirsch, S. R. Wilson and J. S. Moore, *Chem. Eur. J.*, 1997, **3**, 765; K. A. Hirsch, S. R. Wilson and J. S. Moore, *Chem. Commun.*, 1998, 13; L. Carlucci, G. Ciani, D. Proserpio and A. Sironi, *J. Am. Chem. Soc.*, 1995, **117**, 4562; L. Carlucci, G. Ciani, D. Proserpio and A. Sironi, *Chem. Commun.*, 1996, 1393.
- 3 M. Fujita, in *Comprehensive Supramolecular Chemistry*, Series ed. J.-M. Lehn, Volume eds. J. L. Atwood, J. E. D. Davies, D. D. MacNicol and F. Vögtle, Pergamon, Oxford, 1996, vol. 9, pp. 253–282; M. Fujita, *Chem. Soc. Rev.*, 1998, **27**, 417; P. J. Stang and B. Olenyuk, *Acc. Chem. Res.*, 1997, **30**, 502; C. J. Jones, *Chem. Soc. Rev.*, 1998, **27**, 289.
- 4 J. P. Collman, L. S. Hegedus, J. R. Norton and R. G. Finke, *Principles and Applications of Organotransition Metal Chemistry*, University Science Books, Mill Valley, CA, 1987; Ch. Elschenbroich and A. Salzer, *Organometallics: A Concise Introduction*, VCH, Weinheim, 2nd edn., 1992.
- 5 For example, see: A. Solladié-Cavallo, *Polyhedron*, 1985, **4**, 901; F. Rose-Munch and E. Rose, *Curr. Org. Chem.*, 1999, **3**, 445; M. F. Semmelhack, in *Comprehensive Organometallic Chemistry II*, eds. E. Abel, F. G. A. Stone and G. Wilkinson, Pergamon, Oxford, 1995, vol. 12, p. 979.
- 6 (a) G. R. Desiraju, *Crystal Engineering: The Design of Organic Solids*, Elsevier, New York, 1989; (b) M. C. Etter, *Acc. Chem. Res.*, 1990, **23**, 120; (c) F. H. Allen, W. D. S. Motherwell, P. R. Raithby, G. P. Shields and R. Taylor, *New J. Chem.*, 1999, **23**, 25.

- 7 For crystal structures of benzoic acid, terephthalic acid isophthalic acid and trimesic acid, see refs. 7a, (7b,c), (7d,e) and 7f, respectively; (a) R. Feld, M. S. Lehman, K. W. Muir and J. C. Speakman, *Z. Kristallogr.*, 1981, **157**, 215; (b) M. Bailey and C. J. Brown, *Acta Crystallogr.*, 1967, **22**, 387; (c) A. Domenicano, G. Schultz, I. Hargittai, M. Colapietro, G. Portalone, P. George and C. W. Bock, *Struct. Chem.*, 1990, **1**, 107; (d) R. Alcalá and S. Martínez-Carrera, *Acta Crystallogr., Sect. B*, 1972, **28**, 1671; (e) J. L. Derissen, *Acta Crystallogr., Sect. B*, 1974, **30**, 2764; (f) F. H. Herbstein, in *Comprehensive Supramolecular Chemistry*, eds. D. D. MacNicol, F. Toda and R. Bishop, Pergamon, Oxford, UK, vol. 6, ch. 3, 1996 and references therein.
- 8 The term *supramolecular synthon*, is hereafter contracted to *synthon*, see: G. R. Desiraju, *Angew. Chem., Int. Ed. Engl.*, 1995, **34**, 2311; (b) for a review of graph set nomenclature for classifying hydrogen bonds, see: J. Bernstein, R. E. Davis, L. Shimoni and N.-L. Chang, *Angew. Chem., Int. Ed. Engl.*, 1995, **34**, 1555.
- 9 (a) C. B. Aakeröy and A. M. Beatty, *Chem. Commun.*, 1998, 1067; (b) C. B. Aakeröy, A. M. Beatty and D. S. Leinen, *J. Am. Chem. Soc.*, 1998, **120**, 7383; (c) C. B. Aakeröy and A. M. Beatty, *Cryst. Eng.*, 1998, **1**, 39.
- 10 (a) F. Jaber, F. Charbonnier, R. Faure and M. Petit-Ramel, *Z. Kristallogr.*, 1994, **209**, 536. In related substituted nicotinic acid analogues it has been shown that unpredictability can arise due to silver carboxylate (Ag–O) bond formation. See: (b) C. B. Aakeröy and A. M. Beatty, *J. Mol. Struct.*, 1999, **474**, 91.
- 11 J. C. Mareque Rivas and L. Brammer, *New J. Chem.*, 1998, **22**, 1315.
- 12 R. Atencio, L. Brammer, S. Fang and F. C. Pigge, *New J. Chem.*, 1999, **23**, 461.
- 13 See synthesis of $[\text{Pt}(\text{NC}_5\text{H}_5)_4]^{2+}$, in *Gmelin Handbuch der Anorganische Chemie*, Verlag Chemie, Weinheim, 1957, vol. 68D.
- 14 A. D. Hunter, V. Mozoi and S. T. Tsai, *Organometallics*, 1992, **11**, 2251.
- 15 A. D. Hunter, L. Shilliday, W. S. Furey and M. J. Zaworotko, *Organometallics*, 1992, **11**, 1550.
- 16 SHELXTL 5.0, Bruker (Siemens) Analytical X-Ray Instruments, Inc., 1995.
- 17 (a) G. M. Sheldrick, SADABS, Empirical absorption correction program, University of Göttingen, 1995, based upon the method of Blessing;^{17b} (b) R. H. Blessing, *Acta Crystallogr., Sect. A*, 1995, **51**, 33.
- 18 A channel of solvated chloride ions has recently been reported in the crystal structure of a copper coordination polymer: C. Janiak, T. G. Scharmann, W. Günther, W. Hinrichs and D. Lentz, *Chem. Ber.*, 1996, **129**, 991.
- 19 (a) See, J. C. Mareque Rivas, Ph.D. Thesis, University of Missouri–St. Louis, 1999 for further details; (b) cell dimensions: $a = 11.9622(1)$, $b = 11.9510(1)$, $c = 45.7593(2)$ Å, $\beta = 90.073(1)^\circ$, $V = 6541.8(1)$ Å³ at 213(5) K. $R1 = 0.069$, $wR2 = 0.195$. Refined as monoclinic, space group $I2$, with numerous restraints applied.
- 20 In fact the chloride ligands lie off axis in **1** by 9° , but precisely on axis in $3 \cdot 7\text{H}_2\text{O}$.^{19a}
- 21 C, H, N elemental analysis of the crystals suggests a formula consistent with $3 \cdot 8\text{H}_2\text{O}$, but the crystallographic model did not suggest inclusion of an additional water molecule.
- 22 C. B. Aakeröy, A. M. Beatty and D. S. Leinen, *Angew. Chem., Int. Ed.*, 1999, **38**, 1815.
- 23 V. A. Russell, C. Evans, W. Li and M. D. Ward, *Science*, 1997, **276**, 575.
- 24 (a) M. A. S. Goher and T. C. W. Mak, *Inorg. Chim. Acta*, 1985, **101**, L27; (b) CSD REFCODES: BADHAP, BADXIX, BADKAS, TEXFEH; (c) M. H. Chou, D. J. Szalda, C. Creutz and N. Sutin, *Inorg. Chem.*, 1994, **33**, 1674; (d) two other published structures not yet in the CSD also contain such amide–amide interactions;^{9c,24e} (e) C. B. Aakeröy, A. M. Beatty, D. S. Leinen and K. R. Lorimer, *Chem. Commun.*, 2000, 935; (f) CSD REFCODES: DISFIU, FUWGIN, GOKMAU, NUSGOX, NUSGUD; (g) CSD REFCODES: BEXPAU10, BEXPEZ10, ISNARU, JOSDAW01, KULSEG, TANCRU.
- 25 (a) A. D. Burrows, C.-W. Chan, M. M. Chowdhry, J. E. McGrady and D. M. P. Mingos, *Chem. Soc. Rev.*, 1995, **24**, 329; (b) A. D. Burrows, S. Menzer, D. M. P. Mingos, A. J. P. White and D. J. Williams, *J. Chem. Soc., Dalton Trans.*, 1997, 4237; (c) M. T. Allen, A. D. Burrows and M. F. Mahon, *J. Chem. Soc., Dalton Trans.*, 1999, 215; (d) A. D. Burrows, R. W. Harrington and M. F. Mahon, *CrystEngComm.*, 2000, 12.
- 26 A. S. Batsanov, M. J. Begley, M. W. George, P. Hubberstey, M. Munakata, C. E. Russell and P. H. Walton, *J. Chem. Soc., Dalton Trans.*, 1999, 4251.
- 27 Z. Q. Qin, M. C. Jennings, R. J. Puddephatt and K. W. Muir, *CrystEngComm.*, 2000, 11.

- 28 D. Braga, F. Grepioni, P. Sabatino and G. R. Desiraju, *Organometallics*, 1994, **13**, 3532; see also work on $[\text{Co}(\eta^5\text{-C}_5\text{H}_4\text{COOH})(\eta^5\text{-C}_5\text{H}_4\text{COO})]$ in D. Braga, L. Maini, M. Polito and F. Grepioni, *Organometallics*, 1999, **18**, 2577.
- 29 M. M. Kubicki, P. Richard, B. Gautheron, M. Viotte, S. Toma, M. Hudecek and V. Gajda, *J. Organomet. Chem.*, 1994, **476**, 55.
- 30 D. Braga, F. Grepioni and G. R. Desiraju, *Chem. Rev.*, 1998, **98**, 1375; D. Braga and F. Grepioni, *Acc. Chem. Rev.*, 1997, **30**, 81; D. Braga and F. Grepioni, *J. Chem. Soc., Dalton Trans.*, 1999, 1.
- 31 J. C. Mareque Rivas and L. Brammer, *Coord. Chem. Rev.*, 1999, **183**, 43.
- 32 This nomenclature summarizes the sequence of hydrogen bond donor (D) and acceptor (A) groups on each of the two interacting molecules, see ref. 25(a) for more details.
- 33 A. J. Bondi, *J. Chem. Phys.*, 1964, **68**, 441.
- 34 S. Valiyaveetil, V. Enkelmann and K. Müllen, *J. Chem. Soc., Chem. Commun.*, 1994, 2097.
- 35 F. H. Herbstein and R. E. Marsh, *Acta Crystallogr., Sect. B*, 1977, **33**, 2358; S. V. Kolotuchin, E. E. Fenlon, S. R. Wilson, C. J. Loweth and S. C. Zimmerman, *Angew. Chem., Int. Ed. Engl.*, 1995, **34**, 2654.
- 36 G. R. Desiraju and T. Steiner, *The Weak Hydrogen Bond*, Oxford University Press, London, 1999.